

- [12] Immersion Lamp TQ 150 of Heraeus Noblelight GmbH; power consumption 150 W. The experimental setup is available as Supporting Information.
- [13] P. T. Beurskens, G. Beurskens, M. Strumpel, C. E. Nordman in *Patterson and Pattersons* (Eds.: J. P. Glusker, B. K. Patterson, M. Rossi), Clarendon Press, Oxford, **1987**, p. 356.
- [14] DIRDIF-96, a computer program system for crystal structure determination by Patterson methods and direct methods applied to difference structure factors: P. T. Beurskens, G. Beurskens, W. P. Bosman, R. de Gelder, S. García-Granda, R. O. Gould, R. Israël, J. M. M. Smits, Crystallography Laboratory, University of Nijmegen, The Netherlands, **1996**.
- [15] PLATON-93, program for display and analysis of crystal and molecular structures: A. L. Spek, University of Utrecht, The Netherlands, **1995**.

Paramagnetic Keplerate “Necklaces” Synthesized by a Novel Room-Temperature Solid-State Reaction: Controlled Linking of Metal-Oxide-Based Nanoparticles**

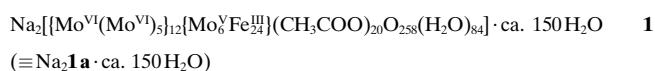
Achim Müller,* Samar K. Das, Marina O. Talismanova,
Hartmut Bögge, Paul Kögerler, Marc Schmidtman,
Sergei S. Talismanov, Marshall Luban, and
Erich Krickemeyer

*Dedicated to Professor C. N. R. Rao on the occasion of the
Silver Jubilee of his Solid State and Structural Chemistry Unit*

The search for extended structures based on linked nano-sized stable building blocks especially with well-defined electronic and magnetic properties is an extremely worthy task because such multidimensional networks could result in new types of functionalized materials.^[1] In this context we are involved in the synthesis of ever larger well-defined metal-oxide-based nanoparticles with unique host properties and their linking through M–O–M- or M–O–M'-type bonds to obtain a wide range of architectures.^[2] For instance, spherical metal-oxide-based Keplerate-type clusters with icosahedral symmetry, which exhibit an internal cavity (diameter) large

enough to even encapsulate Keggin-type clusters—thus leading to remarkable composites—can be generated in a facile synthesis.^[3] The Keplerate-type clusters also display interesting topologies.^[4] So far there has been no report on the linking of such large spherical objects to form a chain structure (for very interesting fullerene-type systems see ref. [5]). Here we report the synthesis and structure of an unusual mixed-valence compound^[6] containing discrete {Mo^{VI}(Mo^{VI})₅}{Mo^VFe^{III}}_{12}-type Keplerate clusters and their one-dimensional linking by a novel type of solid-state reaction at room temperature to form chains. We also present a theoretical model based on a modification of a {Mo^{VI}(Mo^{VI})₅}{Fe^{III}}_{30} prototype^[7] that helps to explain the measured magnetic properties of the chain compound.

If a strongly acidified aqueous solution of sodium molybdate is treated with ferrous chloride in the presence of air and a rather high concentration of acetic acid, black crystals of **1** containing {Mo^{VI}(Mo^{VI})₅}{Mo^VFe^{III}}_{12}-type anionic clusters precipitate, which upon drying at room temperature get linked to chains, yielding (the black) compound **2** (see also Experimental Section).



During the formation process, the Fe^{II} ions partly reduce the Mo^{VI} centers though most of the Fe^{II} cations are oxidized by air to Fe^{III}. In any case the presence of Fe^{II} is necessary, as beginning the synthesis with Fe^{III} as starting material in the presence of a reducing agent leads immediately to a non-crystalline precipitate.

Whereas compound **2** was characterized to a full extent by elemental analysis, thermogravimetry (to determine the crystal water content), bond valence sum (BVS) calculations,^[8] spectroscopic methods (IR, resonance Raman, VIS-NIR, ⁵⁷Fe Mössbauer) as well as magnetic measurements and single-crystal structure analysis,^[9] compound **1**, which contains discrete spherical clusters, could only be identified by single-crystal X-ray structure analysis of the non-dried crystals. These crystals were cooled immediately to liquid nitrogen temperature to block any further release of water and subsequent condensation reactions which would lead to the formation of **2**.^[9]

Both the spherical cluster anion **1a** and the spherical building blocks of the anion chain **2a** comprise 12 pentagonal fragments of the type {Mo^{VI}(Mo^VO₂₁)} (containing a central pentagonal MoO₇ bipyramid edge-sharing with five {MoO₆} octahedra) which are connected by 24 {Fe^{III}(H₂O)₂}³⁺^[10] and six {Mo^VO(H₂O)}³⁺ linkers (the six Mo(4d) electrons are also partially delocalized over the Mo positions of the pentagonal {Mo(Mo₅)} building groups, cf. ref. [11]) statistically distributed over the 30 vertices of an icosidodecahedron. The acetate ligands are located inside the sphere and are coordinated in a bidentate fashion to the metal centers, preferentially bridging Fe and Mo sites. In crystals of **2** the icosahedral spherical building blocks, that is {Mo(Mo)₅}{Mo₆Fe₂₄}-type spheres,

[*] Prof. Dr. A. Müller, Dr. S. K. Das, Dipl.-Chem. M. O. Talismanova, Dr. H. Bögge, Dr. P. Kögerler, M. Schmidtman, Dipl.-Chem. S. S. Talismanov, E. Krickemeyer
Lehrstuhl für Anorganische Chemie I
Fakultät für Chemie, Universität Bielefeld
Postfach 100131, 33501 Bielefeld (Germany)
Fax: (+49) 521-106-6003
E-mail: a.mueller@uni-bielefeld.de
Dr. P. Kögerler, Prof. Dr. M. Luban
Ames Laboratory and Department of Physics and Astronomy
Iowa State University
Ames, IA 50011-3160 (USA)

[**] We thank Prof. A. X. Trautwein and Dr. V. Schünemann, Medizinische Universität zu Lübeck (Germany), for measuring the Mössbauer spectra. M.O.T. thanks the Alfred Töpfer Foundation for her fellowship. This work was supported by the Deutsche Forschungsgemeinschaft and the Fonds der Chemischen Industrie. The Ames Laboratory is operated for the United States Department of Energy by Iowa State University under Contract No. W-7405-Eng-82.

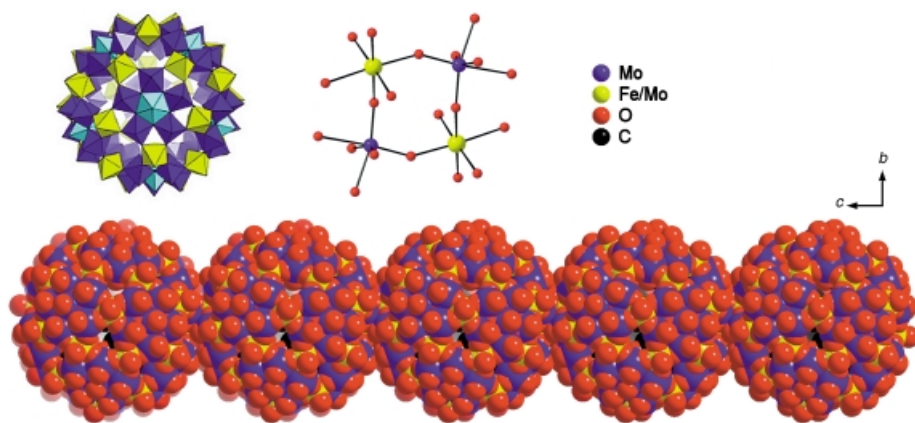
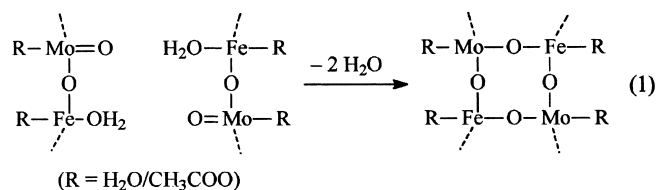


Figure 1. Representation of the structures of the discrete anion **1a** in crystals of **1** (polyhedra), of the anionic chain **2a** in crystals of **2** (space-filling with the option to identify the Mo positions), as well as of the linking area of the chain **2a** (ball-and-stick; bond lengths [Å] and angles [°] in the M_4O_4 ($M = \text{Mo/Fe}$) ring: Mo–O: 1.72/1.78; Fe–O: 1.96/1.98; Mo–O–Fe: 147.0/149.9; O–Mo–O: 101.5; O–Fe–O: 93.2).

are linked to form chains (Figure 1): Two neighboring spheres A and B are connected by a $\text{Mo}_A\text{--O--Fe}_B$ and a $\text{Fe}_A\text{--O--Mo}_B$ group, for which the two metal positions of each sphere (e.g., Fe_A and Mo_A) are connected by a μ -oxo-type center. This results in a nearly square Fe_2Mo_2 arrangement (Figure 1 top right), the center of which coincides with a crystallographic inversion center (see below for the type of mechanism). Interestingly, the geometric details of the Fe–O–Mo bridging group and the Fe–O–Mo motifs found in the spheres do not differ significantly ($\text{Mo}\cdots\text{Fe}$: ca. 3.6 Å). This has important implications for the magnetic properties as described below. The square-type linking group in **2** (Figure 1) is topologically equivalent to the type of linking found in dumbbell-shaped $\{\text{C}_{60}\}_2$ dimers, for which the linking region can be compared with a cyclobutane unit built up by two intra- and two inter-sphere C–C bonds.^[5c]

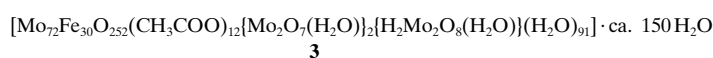
The formation of **2** is initiated by drying crystals of **1**, that is by the loss of crystal water and finally results in the condensation of the anionic cluster spheres so as to link the spheres as infinite chains through the above-described bridging motifs. This is caused by the fact that $\{\text{Fe}^{\text{III}}(\text{H}_2\text{O})_2\}^{3+}$ -type H_2O ligands are substituted by terminal Mo=O groups of $\{\text{Mo}(\text{Mo}_5)\}$ pentagons of neighboring spheres formally acting as ligands in accordance with Equation (1).

The driving force for the reaction is entropy gained by emission of water molecules. The initial loss of crystal water molecules causes decreasing inter-sphere distances, which leads to the situation that an Mo=O group formally acts as a ligand while replacing a H_2O group of an adjacent sphere as mentioned above. This S_N -type reaction initiated by an Mo=O group does not occur for the yellow neutral discrete $\{\text{Mo}^{\text{VI}}(\text{Mo}_5^{\text{VI}})\}_{12}\{\text{Fe}_3^{\text{III}}\}$ -type cluster found in **3**^[7] but in the present case due to the increase in electron density in **1a** at the



terminal Mo=O oxygen positions by the abundance of six (partially delocalized) 4d electrons which cause also the dark color. Remarkably the binuclear Mo_2^{VI} -type linkers of **3** (responsible for the neutrality of the cluster) are not abundant in **1** and **2** due to the different preparation method used here.

Interestingly, not only the crystallinity but also the space group ($P2_1/n$) is preserved throughout the solid-state reaction **1** \rightarrow **2**. Comparing the packing of the spheres in the crystal lattice of **2** with that of **1** reveals that the distances between the $\{\text{Mo}(\text{Mo}_5)\}_{12}$ - $\{\text{Mo}_6\text{Fe}_{24}\}$ -type ball units shrink drastically in the direction of the crystallo-



graphic c axis (Figure 2): Correspondingly, the c axis of **2** is even 5.7 Å shorter than the corresponding one of **1** (see ref. [9]).

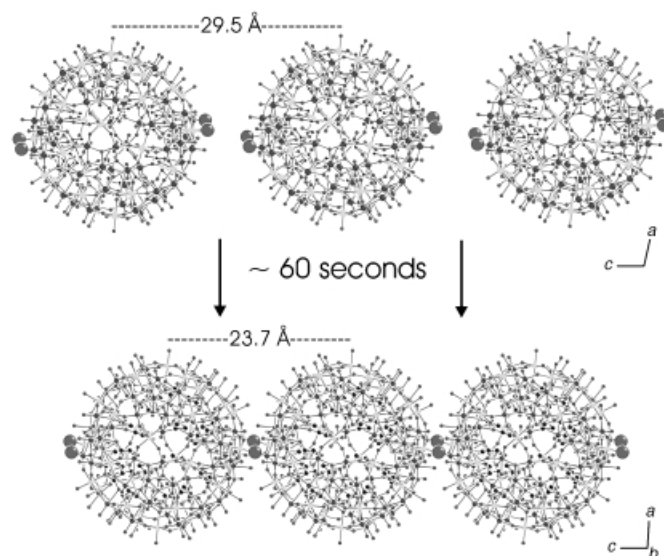


Figure 2. Schematic demonstration of the room-temperature solid-state reaction leading to the chain of **2** caused by linking the anionic spheres **1a**.

The magnetism of **2** can be best explained by comparing it with the prototypical case of the analogous discrete $\{\text{Mo}_7^{\text{VI}}\text{Fe}_{30}^{\text{III}}\}$ spheres of **3**,^[7] currently the largest molecular mesoscopic paramagnet.^[12] In both systems O–Mo–O groups mediate antiferromagnetic exchange between the near-perfect octahedrally coordinated $S = 5/2$ Fe^{III} centers (see also Mössbauer data). In the case of **3**, $\chi_{\text{mol}}T$ increases with T and at room temperature approaches the value expected for 30 uncorrelated $S = 5/2$ centers, namely 131.25 emu K mol^{-1} (spin-only for $g = 2.0$), while the room-temperature value of $\chi_{\text{mol}}T$ found for **2**, 104.0 emu K mol^{-1} , very nearly equates to the expected value for 24 uncorrelated $S = 5/2$ Fe^{III} centers, namely

105.0 emu K mol⁻¹.^[13] As the (partially) delocalized Mo(4d) electrons are, like in the reduced {Mo₁₀₂}-type Keplerate,^[11] strongly coupled and thus contribute only to a negligible extent to the overall magnetic moment, the high-temperature data indicate that in **2** six of the 30 Fe^{III} positions in **3** are occupied by (effectively) nonmagnetic centers. Down to low temperatures the measured susceptibility of both **2** and **3** (Figure 3) are in very good agreement with the Curie–Weiss function $\chi = C/(T - \Theta)$ but the derived Weiss temperatures

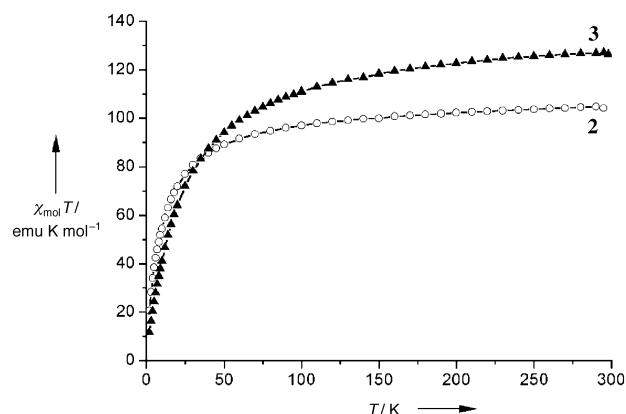


Figure 3. The temperature dependence of $\chi_{\text{mol}}T$ compared for **2** and **3**.

differ significantly ($\Theta(\mathbf{2}) = -13$ K, $\Theta(\mathbf{3}) = -21.6$ K, using susceptibility data extending from 20–300 K).^[12, 14a] The value of the ratio $\Theta(\mathbf{2})/\Theta(\mathbf{3})$ can be explained by adopting the following simple picture. The same single Heisenberg exchange constant J is assumed for the nearest neighbor Fe...Fe interactions in **2** and **3** since the geometrical parameters of the relevant Fe–O–Mo–O–Fe groups including the bridges between the spheres are virtually identical. It then follows that Θ is proportional to the absolute number of nearest neighbor Fe...Fe contacts per sphere,^[15] which in **2** is decreased in comparison to **3** by the introduction of six centers that are effectively not contributing to the paramagnetism, that is, (effectively) nonmagnetic. Assuming a uniform statistical distribution of these nonmagnetic centers over the 30 icosidodecahedron vertices results in 38 Fe...Fe contacts compared to the 62 contacts of a hypothetical all-iron configuration (60 icosidodecahedron edges and two distinct bridges to the adjoining spheres in the chain). We therefore obtain $\Theta(\mathbf{2}) = 38/62 \times \Theta(\mathbf{3}) = -13.2$ K, in excellent agreement with the experimentally determined value. It is noteworthy that, because the Weiss temperature reflects the ordering and the distribution of the nonmagnetic positions over all 30 possible positions, we are able to draw structural conclusions that cannot be obtained from the X-ray diffraction analysis or other analytical techniques.^[14b] Future investigations will center on the low-temperature/high-field regime. In particular, we will probe whether a highly symmetric frustrated ground-state configuration is achieved for **2** as occurs in compound **3**.^[12]

The results reported here focus on several interesting aspects. Nanosized spherical capsule-type objects get linked as one-dimensional chain structures in a room-temperature solid-state reaction, which can be regarded as a type of crystal

engineering process. Additionally, the capsule itself, that is the building block has interesting properties for materials science.^[3] Another important feature is that we deal with spherical capsules of the type (pentagon)₁₂(linker)₃₀ ($L = \text{Fe}(\text{H}_2\text{O})^{3+}$,^[7] $\text{MoO}(\text{H}_2\text{O})^{3+}$ ^[11]) where the linkers can be stepwise exchanged with the option of changing the surface properties for different purposes. For example, by changing appropriately the degree of electron density on the surface (that is, in the present case, by the number of $\text{MoO}(\text{H}_2\text{O})^{3+}$ groups), the nucleophilicity can correspondingly be increased thus, for instance, enabling different types of inter-sphere condensation reactions. The type of linking depends on the $\text{MoO}^{3+}/\text{Fe}^{\text{III}}$ ratio. Furthermore, there is an interesting electronic structure based on the two couples $\text{Fe}^{\text{II}}-\text{Mo}^{\text{VI}}$ and $\text{Fe}^{\text{III}}-\text{Mo}^{\text{V}}$ which have very close redox potentials. Therefore the actual type of electronic structure can lead to temperature-dependent electron transfer in anion **2a**.^[16, 17] Finally, the specific reaction type as well as the resulting products reported here are just one of a myriad of possibilities that appear achievable in future investigations with this system.

Experimental Section

1: $\text{FeCl}_2 \cdot 4 \text{H}_2\text{O}$ (0.5 g, 2.51 mmol) was added to a solution of $\text{Na}_2\text{MoO}_4 \cdot 2 \text{H}_2\text{O}$ (3.0 g, 12.40 mmol) in H_2O (25 mL) and CH_3COOH (100%; 10 mL). After acidification with 32% HCl (2.0 mL) the solution was stirred for 10 min at room temperature and the resulting blue solution was filtered from the blue precipitate and kept in a 100 mL Erlenmeyer flask at 20 °C. After one day, the solution was filtered again. The black crystals (plates or “rhombic” shaped prisms), precipitated after three days, were directly characterized while still wet by single-crystal X-ray structure analysis after they had been extracted from the mother liquor and cooled to liquid nitrogen temperature (otherwise these crystals tend to rapidly lose crystal water).

2: The wet crystals of **1** were filtered, washed with a small amount of cold water, and dried in argon at room temperature. The linking-type reaction based on drying with formation of the chain compound **2** is very fast. Yield: 0.14 g (10% based on Fe). Correct elemental analysis regarding all the elements; but as the Na and C content is very small and the Na^+ ions as well as the acetate groups are partially disordered an error limit regarding their numbers has to be taken into account, that is, a different composition showing, for example, one more Na^+ and acetate cannot be excluded. Characteristic IR bands (KBr pellet; 1800–500 cm⁻¹): $\tilde{\nu} = 1618$ (m, $\delta(\text{H}_2\text{O})$), 1541 (m, $\nu_{\text{as}}(\text{COO})$), 1420 (w-m, $\nu_s(\text{COO})$), 955 (m, $\nu(\text{Mo=O})$), 773 (s), 627 (w-m), 570 (s) cm⁻¹; characteristic resonance Raman bands (solid state; $\lambda_e = 1064$ nm, 1000–200 cm⁻¹): $\tilde{\nu} = 835$ (s), 633 (m), 463 (m-w) cm⁻¹; UV/Vis (solid-state reflectance spectrum, cellulose used as a white standard): $\lambda \approx 390$ (br), 580 (w, br), 850 (w, br), 1064 (w, br) nm; ⁵⁷Fe Mössbauer spectrum (77 K; isomer shift and quadrupole splitting characteristic for Fe^{III}O₆-type groups, in mm s⁻¹): $\delta = 0.52$, $\Delta E_Q = 0.77$.

Received: August 31, 2001 [Z17829]

- [1] A. K. Cheetham, G. Férey, T. Loiseau, *Angew. Chem.* **1999**, *111*, 3466–3492; *Angew. Chem. Int. Ed.* **1999**, *38*, 3268–3292.
- [2] a) A. Müller, P. Kögerler, C. Kuhlmann, *Chem. Commun.* **1999**, 1347–1358; b) A. Müller, P. Kögerler, H. Bögge, *Struct. Bonding (Berlin)* **2000**, *96*, 203–236; c) A. Müller, H. Reuter, S. Dillinger, *Angew. Chem.* **1995**, *107*, 2505–2539; *Angew. Chem. Int. Ed.* **1995**, *34*, 2328–2361.
- [3] A. Müller, S. K. Das, P. Kögerler, H. Bögge, M. Schmidtman, A. X. Trautwein, V. Schünemann, E. Krickemeyer, W. Preetz, *Angew. Chem.* **2000**, *112*, 3555–3559; *Angew. Chem. Int. Ed.* **2000**, *39*, 3413–3417.
- [4] Every Keplerate has, essentially by definition, one central point, its *barycenter*—whether or not occupied by an atom—and its atoms are

- organized in one or more spherical shells around this central point, while each symmetry class of atoms forms the set of vertices of a Platonic or a (generalized) Archimedean solid (see: A. Müller, P. Kögerler, A. Dress, *Coord. Chem. Rev.* **2001**, 222, 193–218; O. Delgado, A. Dress, A. Müller, in *Polyoxometalate Chemistry: From Topology via Self-Assembly to Applications* (Eds.: M. T. Pope, A. Müller), Kluwer, Dordrecht **2001**, pp. 69–87).
- [5] For related topics see: a) A. V. Soldatov, G. Roth, A. Dzyabchenko, D. Johnels, S. Lebedkin, C. Meingast, B. Sundqvist, M. Haluska, H. Kuzmany, *Science* **2001**, 293, 680–683 (polymeric C_{70} has been synthesized by treatment of hexagonally packed C_{70} single crystals under moderate hydrostatic pressure); b) H. Brumm, E. Peters, M. Jansen, *Angew. Chem.* **2001**, 113, 2117–2119; *Angew. Chem. Int. Ed.* **2001**, 40, 2069–2071 (a remarkable chain based on C_{70}^{2-}); c) G.-W. Wang, K. Komatsu, Y. Murato, M. Shiro, *Nature* **1997**, 387, 583–586.
- [6] In general, mixed-valence compounds of this type have remarkable electronic properties (see: *Low Dimensional Electronic Properties of Molybdenum Bronzes and Oxides* (Ed.: C. Schlenker), Kluwer, Dordrecht, **1984**).
- [7] A. Müller, S. Sarkar, S. Q. N. Shah, H. Bögge, M. Schmidtman, Sh. Sarkar, P. Kögerler, B. Hauptfleisch, A. X. Trautwein, V. Schünemann, *Angew. Chem.* **1999**, 111, 3435–3439; *Angew. Chem. Int. Ed.* **1999**, 38, 3238–3241; see also: A. Müller, S. K. Das, E. Krickemeyer, P. Kögerler, H. Bögge, M. Schmidtman, *Solid State Sci.* **2000**, 2, 847–854.
- [8] I. D. Brown in *Structure and Bonding in Crystals, Vol. II* (Eds.: M. O'Keeffe, A. Navrotsky), Academic Press, New York, **1981**, pp. 1–30.
- [9] Crystal structure analysis for **1**: $C_{40}H_{528}Fe_{24}Mo_{78}Na_2O_{532}$, $M_r = 18394.1$ g mol $^{-1}$, monoclinic, space group $P2_1/n$, $a = 25.505(1)$, $b = 36.462(2)$, $c = 29.462(1)$ Å, $\beta = 103.556(1)^\circ$, $V = 26635(2)$ Å 3 , $Z = 2$, $\rho = 2.294$ g cm $^{-3}$, $\mu = 2.524$ mm $^{-1}$, $F(000) = 17892$, crystal size: $0.36 \times 0.16 \times 0.12$ mm 3 . Crystals of **1** were removed from the mother liquor and immediately cooled to 183(2) K on a Bruker AXS SMART diffractometer (three-circle goniometer with 1 K CCD detector, Mo K_{α} radiation, graphite monochromator; hemisphere data collection in ω at 0.3° scan width in three runs with 606, 435, and 230 frames ($\phi = 0, 88$ and 180°) at a detector distance of 5.0 cm). A total of 157370 reflections ($0.90 < \theta < 27.01^\circ$) were collected of which 57462 reflections were unique ($R(\text{int}) = 0.0632$). An empirical absorption correction using equivalent reflections was performed with the program SADABS. The structure was solved with the program SHELXS-97 and refined by using SHELXL-93 to $R = 0.0759$ for 34041 reflections with $I > 2\sigma(I)$, $R = 0.1398$ for all reflections; max./min. residual electron density 3.725 and -1.897 e Å $^{-3}$. Crystal structure analysis for **2**: $C_{40}H_{384}Fe_{24}Mo_{78}Na_2O_{460}$, $M_r = 17097.17$ g mol $^{-1}$, monoclinic, space group $P2_1/n$, $a = 25.360(1)$, $b = 36.647(1)$, $c = 23.730(1)$ Å, $\beta = 93.733(1)^\circ$, $V = 22007(2)$ Å 3 , $Z = 2$, $\rho = 2.580$ g cm $^{-3}$, $\mu = 3.032$ mm $^{-1}$, $F(000) = 16452$, crystal size: $0.16 \times 0.16 \times 0.04$ mm 3 . Dried crystals of **2** were cooled to 183(2) K on a Bruker AXS SMART diffractometer (three circle goniometer with 1 K CCD detector, Mo K_{α} radiation, graphite monochromator; hemisphere data collection in ω at 0.3° scan width in three runs with 606, 435, and 230 frames ($\phi = 0, 88$ and 180°) at a detector distance of 5.0 cm). A total of 112815 reflections ($0.98 < \theta < 25.01^\circ$) were collected of which 38737 reflections were unique ($R(\text{int}) = 0.0736$). An empirical absorption correction using equivalent reflections was performed with the program SADABS. The structure was solved with the program SHELXS-97 and refined by using SHELXL-93 to $R = 0.0622$ for 23168 reflections with $I > 2\sigma(I)$, $R = 0.1231$ for all reflections; max./min. residual electron density 3.064 and -1.414 e Å $^{-3}$. (SHELXS/L, SADABS from G. M. Sheldrick, University of Göttingen 1993/97; structure graphics with DIAMOND 2.1 from K. Brandenburg, Crystal Impact GbR, 2001.) CCDC-169551 (**1**) and CCDC-169552 (**2**) contain the supplementary crystallographic data for this paper. These data can be obtained free of charge via www.ccdc.cam.ac.uk/conts/retrieving.html (or from the Cambridge Crystallographic Data Centre, 12, Union Road, Cambridge CB2 1EZ, UK; fax: (+44) 1223-336-033; or deposit@ccdc.cam.ac.uk).
- [10] The abundance of octahedral $Fe^{III}O_6$ groups was also proven by Mössbauer spectroscopy (see Experimental Section). The presence of one $[Mo^{VI}O]^{4+}$ instead of an $[Mo^{VO}]^{3+}$ linker group and the related change of the number of Na atoms cannot be completely excluded within the error limits of the invoked analytical techniques.
- [11] A. Müller, S. Q. N. Shah, H. Bögge, M. Schmidtman, P. Kögerler, B. Hauptfleisch, S. Leiding, K. Wittler, *Angew. Chem.* **2000**, 112, 1677–1679; *Angew. Chem. Int. Ed.* **2000**, 39, 1614–1616.
- [12] a) A. Müller, M. Luban, C. Schröder, R. Modler, P. Kögerler, M. Axenovich, J. Schnack, P. Canfield, S. Bud'ko, N. Harrison, *Chem-PhysChem* **2001**, 2, 517–521; b) M. Luban, J. Schnack, R. Modler, *Europhys. Lett.* **2001**, in press.
- [13] Susceptibility measurements were performed from 2–300 K at 0.5 Tesla using a Quantum Design MPMS-5S and a MPMS-2 SQUID magnetometer.
- [14] a) The nearly perfect agreement with the Curie–Weiss law also rules out the presence of Fe^{II} centers which would result in a significant deviation from the linearity of $1/\chi$ versus T due to temperature-dependent spin-orbit coupling contributions (see, e.g., H. Lueken, *Magnetochemie*, Teubner, Stuttgart **1999**, pp. 246–257). b) It is interesting to compare the present situation of a uniform distribution of (effectively) nonmagnetic positions with other distribution scenarios, for example, maximum clustering of these positions (i.e., all are situated on neighboring sites of the icosidodecahedron), for which the Weiss temperature should change to -18 K. Here, the excellent fit provided by the Curie–Weiss expression in addition indicates the uniform character of the individual spheres with respect to the ratio of the number of magnetic to (effectively) nonmagnetic positions (24:6), whereas a distribution of different ratios with the same average 24:6 ratio would not be accurately characterized by a Curie–Weiss term. By single-crystal X-ray structure analysis it would not be possible to discriminate between the situation of all spherical units having the same composition as in the present case and the situation of the abundance of spheres with different ratios of the magnetic/effectively nonmagnetic linkers but yielding overall the same Fe^{III}/Mo^V average ratio of 24:6.
- [15] This result follows upon inspecting the standard expression for Θ for systems with a single exchange constant, see for example N. W. Ashcroft, N. D. Mernin, *Solid State Physics*, Saunders College, Philadelphia, **1976**.
- [16] An equilibrium $Mo^{VI} + Fe^{II} \leftrightarrow Fe^{III} + Mo^V$ has been anticipated for octahedral sites in metal oxides (see: J. B. Goodenough in *Chemical Uses of Molybdenum, Proc. 4th Int. Conf. on Molybdenum* (Eds.: H. F. Barry, P. C. H. Mitchel), CLIMAX Molybdenum Co., Michigan, **1982**, p. 1). The related electron transfers are analogous to electron delocalization situations in appropriate “heteropoly blues”. This has been supported by quantum-chemical studies of electron transfer transitions of metal-substituted polyoxometalates as well as different Mössbauer data for the cerium salt of 12-molybdophosphoric acid containing 0.6 Fe as counterion and 0.9 Fe^{II} substituted into the Keggin unit obtained at room temperature and low temperatures (4.2 K) (see also S. A. Borshch, H. Duclaud in *Polyoxometalate Chemistry: From Topology via Self-Assembly to Applications* (Eds.: M. T. Pope, A. Müller), Kluwer, Dordrecht, **2001**, pp. 135–144).
- [17] For a related investigation on electron hopping delocalization and trapping in mixed-valence metal–oxygen clusters see H. So, M. T. Pope in *Electron and Proton Transfer in Chemistry and Biology* (Eds.: A. Müller, H. Ratajczak, W. Junge, E. Diemann), Elsevier, Amsterdam **1992**, pp. 71–93, and references therein.